Vertical Lagrangian-remapping, generalized vertical coordinates, and spurious diapycnal mixing in ocean models

COMMODORE Meeting

30 Jan 2020

Hamburg, Germany

STEPHEN.GRIFFIES@NOAA.GOV
ALISTAIR.ADCROFT@NOAA.GOV
ROBERT.HALLBERG@NOAA.GOV

NOAA/GFDL + Princeton University

Key points in this talk

- ⋆ SPURIOUS DIAPYCNAL MIXING: This problem corrupts many state-of-the-science ocean simulations, particularly those for climate where errors accumulate to degrade stratification and contribute to spurious tracer evolution.
- ⋆ DYNAMICAL CORE FORMULATION: The vertical Lagrangian-remap method and generalized vertical coordinate formulation of ocean equations can be understood through basic notions of fluid mechanics.
- ⋆ CONJECTURE: Vertical Lagrangian-remapping with an appropriate hybrid vertical coordinate provides a suitable (perhaps optimal) framework to simulate the ocean climate system without incurring physically disruptive spurious mixing.

  $\longrightarrow$ We are not there yet, but we will show promising results.
- ⋆ ELEMENTS OF THIS TALK ARE TAKEN FROM:
  - *A primer on ocean generalized vertical coordinate dynamical cores based on the vertical Lagrangian-remap method*, 2020: Griffies, Adcroft, and Hallberg, *in review at JAMES*
  - Adcroft et al, 2019: The GFDL Global Ocean and Sea Ice Model OM4.0: Model Description and Simulation Features, *JAMES*.

Outline

1. The spurious numerical diapycnal mixing problem
2. Vertical Lagrangian-remapping w/ generalized vertical coordinates
3. Closing comments

Outline

1. The spurious numerical diapycnal mixing problem

Physically based diapycnal mixing MacKinnon et al (2017)

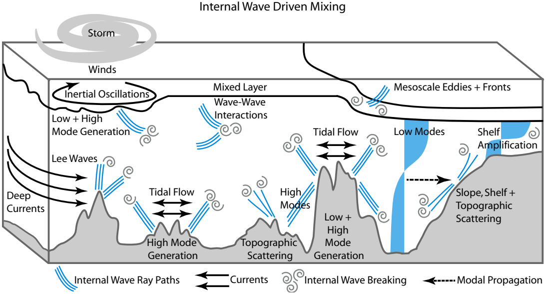

- ⋆ There are many physical sources for ocean diapycnal mixing.
- ⋆ Diapycnal mixing impacts on vertical stratification, dynamics, tracer ventilation (heat, carbon), sea level, with effects more important as time increases (e.g., climate).
- ⋆ Coordinated efforts such as the US Climate Process Team on internal gravity wave mixing (2010-2015) and ongoing German TRR 181 on energetic transfers have enhanced integrity of physically based mixing parameterizations used by climate and prediction models.
- ⋆ Unfortunately, numerical transport (i.e., advection schemes) can introduce spurious diapycnal mixing that is larger than physics.

PRINCETON UNIVERSITY

Framing the spurious mixing problem

The numerical representation of advection $= \nabla \cdot (\rho\, C\, \boldsymbol{v})$ generally introduces spurious mixing and unmixing due to truncation errors

$$\nabla \cdot (\rho\, C\, \boldsymbol{v})_{\text{model}} = \nabla \cdot (\rho\, C\, \boldsymbol{v})_{\text{exact}} + \nabla \cdot (\rho\, C\, \boldsymbol{v})_{\text{error}} \tag{1}$$

- ⋆ Errors in numerical advection can be interpreted as an extra SGS term

$$\frac{\partial(\rho\, C)}{\partial t} + \nabla \cdot (\rho\, C\, \boldsymbol{v})_{\text{exact}} = -\nabla \cdot \left[\boldsymbol{J} + (\rho\, C\, \boldsymbol{v})_{\text{error}}\right]. \tag{2}$$

- ⋆ Error term is not physical nor is it under our direct control. If large it can corrupt physical integrity of the simulation.
- ⋆ Error term can become larger when refine grid spacing to partially resolve mesoscale eddies, which pump tracer variance to the grid scale.
- ⋆ Spurious mixing from the error term is reduced (but not eliminated) when use higher order accurate advection.
- ⋆ Key concern for climate is spurious diapycnal mixing.
- ⋆ Spurious diapycnal mixing is reduced when use quasi-isopycnal vertical coordinate; errors stopped at layer interface.

Diagnosing spurious diapycnal mixing

Griffies, Pacanowski, Hallberg (2000)

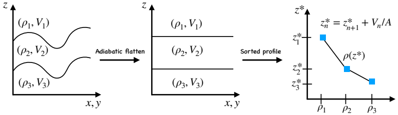

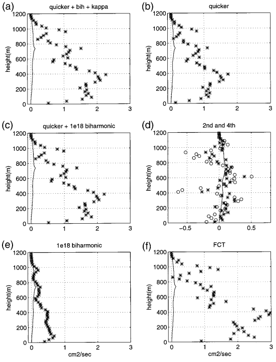

- ⋆ A method based on density sorting to produce a stable background profile, ρ_{back}, following Winters and D'Asaro (1995).
- ⋆ In an adiabatic simulation, evolution of the background state only arises from spurious numerical sources, which we interpret as an effective diffusivity, κ_{eff}

$$\frac{\partial \rho_{\text{back}}}{\partial t} = \frac{\partial}{\partial z^*}\left[\kappa_{eff}\,\frac{\partial \rho_{\text{back}}}{\partial z^*}\right] \tag{3}$$

- ⋆ Diagnosed levels of κ_{eff} from numerical advection can be 10-100x larger than ocean measurements.
- ⋆ Problems can be enhanced in mesoscale eddying simulations where tracer variance is pumped to the gridscale.
- ⋆ Spurious mixing scales with lateral grid Reynolds number (see also Ilicak, Adcroft, Griffies, Hallberg, (2012)):

$$\text{Re}_{\text{grid}} = U\,\Delta t/\Delta < \mathcal{O}(10). \tag{4}$$

Larger Re_{grid} allows for noisy vertical velocity from noisy horizontal convergences: recipe for spurious mixing.

- ⋆ But $\text{Re}_{\text{grid}} > 10$ is very common, thus incurring spurious mixing.

Measures of spurious (diapycnal) mixing

- Sorting along with passive tracer releases
  - Hill, Ferreira, Campin, Marshall, Abernathey, Barrier, 2012: Controlling spurious diapycnal mixing in eddy-resolving height-coordinate ocean models-insights from virtual deliberate tracer release experiments
  - Getzlaff, Nurser, Oschlies, 2012: Diagnostics of diapycnal diffusion in z-level ocean models. Part II: 3-Dimensional OGCM
- BACKGROUND/REFERENCE POTENTIAL ENERGY: Global number (though Ilicak, 2016 suggests local)
  - Ilicak, Adcroft, Griffies, Hallberg, 2012: Spurious dianeutral mixing and the role of momentum closure
  - Petersen, Jacobsen, Ringler, Hecht, Maltrud, 2015: Evaluation of the arbitrary Lagrangian-Eulerian vertical coordinate method in the MPAS-Ocean model
  - Zhao and Liu, 2016: Spurious dianeutral mixing in a global ocean model using spherical centroidal voronoi tessellations
  - Ilicak, 2016: Quantifying spatial distribution of spurious mixing in ocean models
  - Gibson, Hogg, Kiss, Shakespeare, Adcroft, 2017: Attribution of horizontal and vertical contributions to spurious mixing in an Arbitrary Lagrangian-Eulerian ocean model
- VARIANCE METHODS: provides a map for all mixing (no distinction between diapycnal versus isopycnal).
  - Morales-Maqueda and Holloway, 2006: Second-order moment advection scheme applied to Arctic Ocean simulation
  - Burchard, Rennau, 2008: Comparative quantification of physically and numerically induced mixing in ocean models
  - Klingbeil, Mohammadi-Aragh, Grawe, Burchard, (2014): Quantification of spurious dissipation and mixing-discrete variance decay in a Finite-Volume framework
- WATERMASS ANALYSIS
  - Lee, Coward, Nurser 2002: Spurious Diapycnal Mixing of the Deep Waters in an Eddy-Permitting Global Ocean Model
  - Urakawa, Hasumi, 2014: Effect of numerical diffusion on the water mass transformation in eddy-resolving models
  - Megann, 2018: Estimating the numerical diapycnal mixing in an eddy-permitting ocean model
  - Holmes, Zika, England, 2019: Diathermal heat transport in a global ocean model

PRINCETON UNIVERSITY

Some general points emerging from the studies

- ⋆ Diagnosing the spurious mixing is useful for understanding its character but insufficient to remove the problem.
- ⋆ Higher order numerics helps [e.g., Hill et al (2012)], though realistic simulatons need flux limiters that add mixing.
- ⋆ Maintenance of modest grid Reynolds number [$\mathrm{Re}_{\mathrm{grid}} < \mathcal{O}(10)$] is key to suppress velocity noise that translates into spurious mixing [e.g., Ilicak, Adcroft, Griffies, Hallberg (2012)].
- ⋆ Problem arises from advection in both vertical and horizontal (since isopycnals slope) [e.g., Gibson et al (2017)].
- ⋆ Claims that the problem is solved by certain advection schemes [e.g., Hill et al (2012)] have ignored flux limiters, which add mixing and yet are needed to ensure positive definite tracer concentrations [e.g., Morales-Maqueda and Holloway (2006)].
- ⋆ Ilicak et al (2012) and Megann (2018) and Adcroft et al (2019) suggest that 1/4 degree $Z-$coordinate climate models are poorly situated:
  - Admitting mesoscale eddies w/ 1/4-degree generally requires $\mathrm{Re}_{\mathrm{grid}} > \mathcal{O}(10)$.
  - Suggestions (anecdotal) that 1/10-degree Z-model climate simulations have far smaller spurious mixing; perhaps the grid resolves enough of the variance cascade that its dissipation does not require excessive mixing.

PRINCETON UNIVERSITY

Outline

2. Vertical Lagrangian-remapping w/ generalized vertical coordinates

Focusing on the vertical solution method

- ⋆ Isopycnal models have direct control over diapycnal transport.
- ⋆ But isopycnal models are have problems for climate modeling (weakly stratified high latitudes) and coastal (strong vertical mixing).
- ⋆ Hybrid vertical coordinates is a strategy to reduce spurious mixing while allowing for global coverage.
- ⋆ Arbitrary-Lagrangian-Eulerian (ALE) method, including the special case of vertical Lagangian-remapping, is a strategy to realize hybrid vertical coordinates:
  - Leclair, Madec (2011): $\tilde{z}$-Coordinate, an Arbitrary Lagrangian-Eulerian coordinate separating high and low frequency motions provide a case-in-point (see also Petersen et al 2015).
- ⋆ Here we present some of the fundamentals, aiming to develop intuition based on fluid mechanics rather than numerical algorithm details.

PRINCETON UNIVERSITY

Finite volume (weak formulation): Leibniz-Reynolds

$$\frac{\mathrm{d}}{\mathrm{d}t}\left[\int_{\mathcal{R}} \rho\, C \,\mathrm{d}V\right] = -\oint_{\partial\mathcal{R}} \left[\rho\, C\,(\boldsymbol{v} - \boldsymbol{v}^{(b)}) + \boldsymbol{J}\right] \cdot \hat{\boldsymbol{n}}\,\mathrm{d}\mathcal{S}$$

$$\frac{\mathrm{d}}{\mathrm{d}t}\left[\int_{\mathcal{R}} \rho\, \boldsymbol{v} \,\mathrm{d}V\right] = -\int_{\mathcal{R}} [2\,\boldsymbol{\Omega} \wedge \rho\,\boldsymbol{v} + \rho\,\nabla\Phi]\,\mathrm{d}V + \oint_{\partial\mathcal{R}} [-p\,\mathbb{I} - \rho\,\boldsymbol{v} \otimes (\boldsymbol{v} - \boldsymbol{v}^{(b)}) + \mathbb{T}] \cdot \hat{\boldsymbol{n}}\,\mathrm{d}\mathcal{S}$$

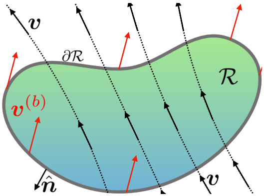

- ⋆ Discrete equations follow by specializing $\mathcal{R}$ to a model grid cell.
- ⋆ Models typically formulate scalar prognostic budgets for extensive quantities: heat, salt, and thus diagnose intensive quantities as in $C = (C\,\rho\,\Delta V)/(\rho\,\Delta V)$.
- ⋆ However, models often formulate a discrete velocity equation, $\partial_t \boldsymbol{v}$, rather than a discrete momentum equation, $\partial_t(\boldsymbol{v}\,\rho\,\Delta V)$, since there are advantages to the vector-invariant velocity equation (e.g., Sadourny energy-enstrophy) over advective-form momentum equation.
- ⋆ Advection refers to the transport of fluid relative to the grid. Fully Lagrangian has zero advection. Fully Eulerian has all motion leading to advection.

GVCs and dia-surface transport (Section 6.7 of Griffies 2004)

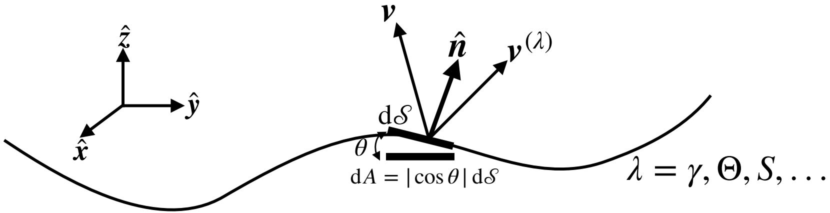

Dia-surface velocity component, u^{dia}, is defined by seawater transport through moving λ surface

$$\mathcal{T} \equiv u^{\text{dia}}\,\mathrm{d}\mathcal{S} \equiv \hat{\boldsymbol{n}} \cdot (\boldsymbol{v} - \boldsymbol{v}^{(\lambda)})\,\mathrm{d}\mathcal{S} \Longrightarrow \text{can have non-zero transport even if } \hat{\boldsymbol{n}} \cdot \boldsymbol{v} = 0. \tag{5}$$

$$\hat{\boldsymbol{n}} = \nabla\lambda\,|\nabla\lambda|^{-1} = \quad \text{normal direction pointing to larger } \lambda. \tag{6}$$

$$\boldsymbol{v} = \text{(barycentric) velocity of fluid element and } \;(\partial_t + \boldsymbol{v}^{(\lambda)} \cdot \nabla)\,\lambda = 0. \tag{7}$$

Following from these definitions we have

$$\frac{\mathrm{D}\lambda}{\mathrm{D}t} = (\partial_t + \boldsymbol{v} \cdot \nabla)\,\lambda = [\partial_t + \boldsymbol{v}^{(\lambda)} \cdot \nabla + (\boldsymbol{v} - \boldsymbol{v}^{(\lambda)}) \cdot \nabla]\,\lambda = 0 + u^{\text{dia}}\,|\nabla\lambda| \tag{8}$$

$$\Longrightarrow |\nabla\lambda|\,u^{\text{dia}} = \frac{\mathrm{D}\lambda}{\mathrm{D}t} = \dot{\lambda} \Longrightarrow \text{material changes in } \lambda \Longleftrightarrow \text{dia-surface transport.} \tag{9}$$

For stably stratified λ-surfaces as in generalized vertical coordinates with $\lambda = \sigma$, we define

$$\mathcal{T} \equiv u^{\text{dia}}\mathrm{d}\mathcal{S} \equiv w^{(\dot{\sigma})}\mathrm{d}A = \frac{\partial z}{\partial \sigma}\,\dot{\sigma} \Longrightarrow \frac{\mathrm{D}}{\mathrm{D}t} = \left[\frac{\partial}{\partial t}\right]_{\sigma} + \boldsymbol{u} \cdot \nabla_{\sigma} + w^{(\dot{\sigma})}\,\frac{\partial}{\partial z} \tag{10}$$

PRINCETON UNIVERSITY

The Arbitrary Lagrangian-Eulerian method (ALE)

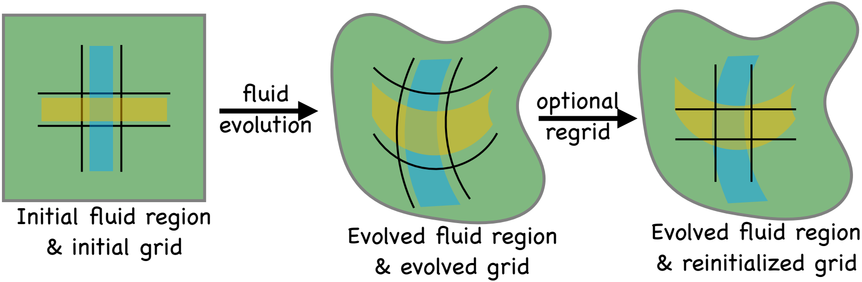

- ⋆ ALE broadly refers to any method that considers moving cell boundaries.
  - ◇ STEP ONE: If grid moves with the flow it is a Lagrangian step. Non-Lagrangian grid motion is also considered by certain ALE approaches.
  - ◇ STEP TWO: The regrid/remap step ideally does not alter the ocean state. Rather, it moves the grid ("regrid") and estimates the ocean state on the new grid ("remap").
- ⋆ Remap step operationally equals to advection (transport relative to grid).
- ⋆ Ocean models restrict their moving meshes to be just in the vertical and formulate equations using generalized vertical coordinates.

Distinguishing solution methods according to $\boldsymbol{v}^{(b)}$

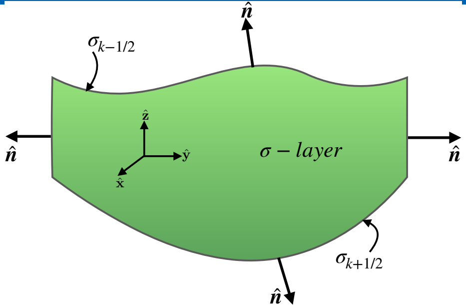

- ⋆ LATERAL BOUNDARIES: $\boldsymbol{v}^{(b)} \cdot \hat{\boldsymbol{n}}_{\text{sides}} = 0$ (no lateral cell movement).
- ⋆ RIGID-LID Z-MODELS: $\boldsymbol{v}^{(b)} \cdot \hat{\boldsymbol{n}} = 0$ for all boundaries.
- ⋆ FREE SURFACE MODELS: $\boldsymbol{v}^{(b)} \cdot \hat{\boldsymbol{n}}_{k=1/2} \neq 0$.
- ⋆ ANALYTICALLY SPECIFIED COORDINATES: barotropic motion specifies $\boldsymbol{v}^{(b)} \cdot \hat{\boldsymbol{n}}_{k\pm1/2} \neq 0$ for $\sigma_{\text{terrain}} = (z - \eta)/(H + \eta), z^* = H\,\sigma_{\text{terrain}}$, others.
- ⋆ ISOPYCNAL LAYERS: $\boldsymbol{v}^{(b)} \cdot \hat{\boldsymbol{n}}_{k\pm1/2} \neq 0$ determined by following layer interfaces.
- ⋆ MORE GENERAL ALE: $\boldsymbol{v}^{(b)} \cdot \hat{\boldsymbol{n}}_{k\pm1/2} \neq 0$ is arbitrary.

Vertical Lagrangian-Remapping method

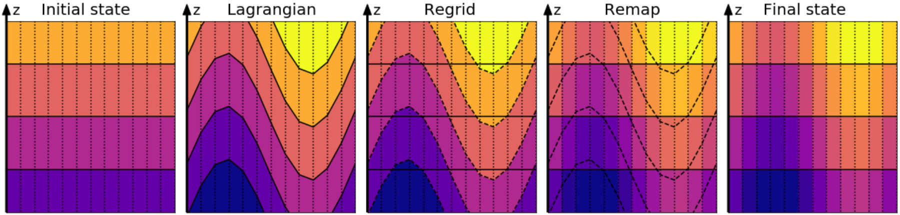

- ⋆ A flavor of ALE where grid cell sides are rigid but top and bottom move.
- ⋆ HYCOM and MOM6 implement the regrid/remap step, constituting the *vertical Lagrangian remap method*.
- ⋆ HYCOM and MOM6 implement the method so that grid layers can vanish and inflate (useful for estuaries and moving ice-shelf grounding lines).
- ⋆ MPAS-O and NEMO algorithms do not implement the vertical regrid/remap step. They are ALE but not Lagrangian.

Comments about vertical Lagrangian-remapping

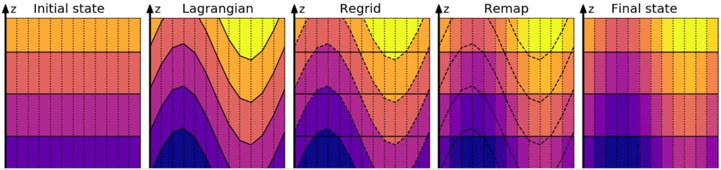

- WHERE IS DIA-SURFACE ADVECTION? It is part of the evolution of the grid cell thicknesses. Cell interfaces move and carry the state.
  - ⋆ Z-COORDINATE EXAMPLE: Define h^* according to fixed z-levels. Remapping moves the state onto the fixed $z-$grid, a step that is the operationally same as vertical advection.
- To diagnose the full advection operator, we need to diagnose the contribution from remapping so that

$$\nabla \cdot (\rho\, C\, \mathbf{v}) = \underbrace{\nabla_\sigma \cdot (\rho\, C\, \boldsymbol{u})}_{\text{horizontal layer advection}} + \text{ remapping.} \quad (11)$$

- There is no CFL associated with vertical remapping; useful for fine vertical grid spacing. But remember stability does not imply accuracy.
- The vertical remapping algorithm can be used for diagnostic purposes to remap and bin grid cell tendencies according to arbitrary surfaces.

Distinguishing three solution algorithms

- ⋆ We consider three solution algorithms used by ocean models:
  - quasi-Eulerian (e.g., MITgcm, MOM5, NEMO)
  - vertical ALE without remapping (e.g., NEMO-$\tilde{z}$, MPAS-O)
  - vertical Lagrangian-remapping (e.g., HYCOM, MOM6)
- ⋆ To exemplify the rudiments of the algorithms, consider the following bare-bones suite of model equations.

$$\frac{\partial \boldsymbol{u}}{\partial t} = \boldsymbol{A} - w^{(\dot{\sigma})} \frac{\partial \boldsymbol{u}}{\partial z} \qquad \text{velocity} \qquad (12a)$$

$$\frac{\partial h}{\partial t} = -\nabla_{\sigma} \cdot (h\,\boldsymbol{u}) - \Delta_{\sigma} w^{(\dot{\sigma})} \qquad \text{thickness} \qquad (12b)$$

$$\frac{\partial (h\,C)}{\partial t} = -\nabla_{\sigma} \cdot [h\,\boldsymbol{u}\,C] - \Delta_{\sigma} [C\,w^{(\dot{\sigma})}] \qquad \text{thickness weighted tracer,} \qquad (12c)$$

where $\boldsymbol{A}$ encompasses accelerations other than dia-surface advection.

Quasi-Eulerian algorithm

- ⋆ Vertical coordinate analytically determined by barotropic motion that then determines thickness tendency as in

$$z^* = \frac{z-\eta}{H+\eta} \Longrightarrow \mathrm{d}z = (1+\eta/H)\,\mathrm{d}z^* \Longrightarrow \partial_t(\mathrm{d}z) = \frac{\mathrm{d}z^*}{H}\,\partial_t\eta. \tag{13}$$

- ⋆ Example codes: MITgcm, MOM5, NEMO-basic, ROMS
- ⋆ There is no realization of this algorithm with vanishing layers that maintains machine precision conservation.

ALGORITHM STEPS

1. $[\Delta_\sigma w^{\text{grid}}]^{(n)} = [\partial h/\partial t]^{(n)} \propto [\partial\eta/\partial t]^{(n)}$ grid motion $\propto$ free surface
2. $h^{(n+1)} = h^{(n)} + \Delta t\,[\Delta_\sigma w^{\text{grid}}]^{(n)}$ update layer thickness
3. $[\Delta_\sigma w^{(\dot\sigma)}]^{(n)} = -[\Delta_\sigma w^{\text{grid}}]^{(n)} - \nabla_\sigma\cdot[h\,\boldsymbol{u}]^{(n)}$ diagnose dia-surface velocity
4. $\boldsymbol{u}^{(n+1)} = \boldsymbol{u}^{(n)} + \Delta t\left[\boldsymbol{A} - w^{(\dot\sigma)}\,\partial\boldsymbol{u}/\partial z\right]^{(n)}$ update horizontal velocity
5. $h^{(n+1)}\,C^\dagger = [h\,C]^{(n)} - \Delta t\,[\nabla_\sigma\cdot(h\,\boldsymbol{u}\,C)]^{(n)}$ incremental tracer step I
6. $h^{(n+1)}\,C^{n+1} = h^{(n+1)}\,C^\dagger - \Delta t\,\Delta_\sigma\left[C^\dagger\,(w^{(\dot\sigma)})^{(n)}\right]$ incremental tracer step II

Algorithm for vertical ALE without remapping

- General thickness tendency with general vertical coordinates.
- Vertical coordinate need not be analytically defined.
- Example codes: MPAS-O and NEMO-$\tilde{z}$
- There is no realization of this algorithm with vanishing layers that maintains machine precision conservation.

ALGORITHM STEPS (ONLY STEP 1 DIFFERS FROM QUASI-EULERIAN)

1. $[\Delta_\sigma w^{\text{grid}}]^{(n)} = (h^{\text{target}} - h^{(n)})/\Delta t$ — general layer motion
2. $h^{(n+1)} = h^{(n)} + \Delta t\, [\Delta_\sigma w^{\text{grid}}]^{(n)}$ — update layer thickness
3. $[\Delta_\sigma w^{(\dot\sigma)}]^{(n)} = -[\Delta_\sigma w^{\text{grid}}]^{(n)} - \nabla_\sigma \cdot [h\,\boldsymbol{u}]^{(n)}$ — diagnose dia-surface velocity
4. $\boldsymbol{u}^{(n+1)} = \boldsymbol{u}^{(n)} + \Delta t \left[\boldsymbol{A} - w^{(\dot\sigma)}\, \partial \boldsymbol{u}/\partial z\right]^{(n)}$ — update horizontal velocity
5. $h^{(n+1)}\, C^{\dagger} = [h\, C]^{(n)} - \Delta t\, [\nabla_\sigma \cdot (h\,\boldsymbol{u}\, C)]^{(n)}$ — incremental tracer step I
6. $h^{(n+1)}\, C^{n+1} = h^{(n+1)}\, C^{\dagger} - \Delta t\, \Delta_\sigma \left[C^{\dagger}\, (w^{(\dot\sigma)})^{(n)}\right]$ — incremental tracer step II

PRINCETON UNIVERSITY

Vertical Lagrangian-remapping algorithm

- Pioneered by Bleck (2002).
- General thickness tendency with general vertical coordinates.
- Vertical coordinate need not be analytically defined.
- Lagrangian step includes horizontal dynamics/physics + vertical physics
- Example codes: HYCOM and MOM6
- MOM6 allows for vanishing layers with machine precision conservation.

ALGORITHM STEPS

1. $[\Delta_\sigma w^{\text{grid}}]^{(n)} = -\nabla_\sigma \cdot [h\,\boldsymbol{u}]^{(n)}$ layer motion as per horizontal convergence
2. $h^\dagger = h^{(n)} + \Delta t\,[\Delta_\sigma w^{\text{grid}}]^{(n)}$ Lagrangian thickness
3. $[\Delta_\sigma w^{(\dot\sigma)}]^{(n)} = 0$ zero dia-surface velocity
4. $\boldsymbol{u}^\dagger = \boldsymbol{u}^{(n)} + \Delta t\,\boldsymbol{A}^{(n)}$ Lagrangian velocity
5. $h^\dagger\,C^\dagger = h^{(n)}\,C^{(n)} - \Delta t\,[\nabla_\sigma \cdot (h\,C\,\boldsymbol{u})]^{(n)}$ Lagrangian tracer
6. $h^{(n+1)} = h^{\text{target}}$ regrid to the target
7. $\Delta_\sigma w^{(\dot\sigma)} = -(h^{\text{target}} - h^\dagger)/\Delta t$ dia-surface velocity
8. $\boldsymbol{u}^{(n+1)} = \boldsymbol{u}^\dagger + \Delta t\,w^{(\dot\sigma)}\,(\partial \boldsymbol{u}^\dagger/\partial z)$ remap velocity
9. $h^{(n+1)}\,C^{(n+1)} = h^\dagger\,C^\dagger - \Delta t\,\Delta_\sigma(w^{(\dot\sigma)}\,C^\dagger)$ remap tracer.

Scalar equations for algorithms without remapping

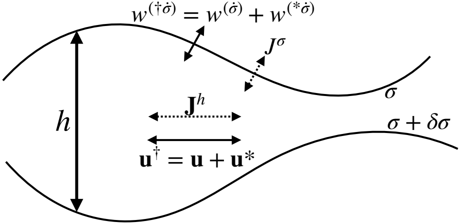

- ⋆ Resolved vertical velocity, $w^{(\dot{\sigma})}$, and parameterized vertical velocity (e.g., eddy-induced velocity), $w^{(*\dot{\sigma})}$, are diagnosed via continuity equations.
- ⋆ Both $w^{(\dot{\sigma})}$ & $w^{(*\dot{\sigma})}$ penetrate layer interfaces as per traditional advection.

$$\frac{\partial(h\,\rho)}{\partial t} + \nabla_{\sigma}\cdot(h\,\rho\,\boldsymbol{u}^{\dagger}) + \delta_{\sigma}(\rho\,w^{(\dagger\dot{\sigma})}) = 0 \quad \text{and} \quad \nabla_{\sigma}\cdot(h\,\rho\,\boldsymbol{u}^{*}) + \delta_{\sigma}(\rho\,w^{(*\dot{\sigma})}) = 0 \qquad (14)$$

$$\frac{\partial(h\,\rho\,C)}{\partial t} + \nabla_{\sigma}\cdot(h\,\rho\,C\,\boldsymbol{u}^{\dagger}) + \delta_{\sigma}(\rho\,C\,w^{(\dagger\dot{\sigma})}) = -\left[\nabla_{\sigma}\cdot(h\,\boldsymbol{J}^{h}) + \delta_{\sigma}J^{\sigma}\right] \qquad (15)$$

$$z_{\sigma} = \frac{\partial z}{\partial\sigma} \qquad h = z_{\sigma}\,\mathrm{d}\sigma \qquad w^{(\dagger\dot{\sigma})} = \frac{\partial z}{\partial\sigma}\frac{\mathrm{D}^{\dagger}\sigma}{\mathrm{D}t} = w^{(\dot{\sigma})} + \boldsymbol{v}^{*}\cdot z_{\sigma}\nabla\sigma = w^{(\dot{\sigma})} + w^{(*\dot{\sigma})} \qquad (16)$$

$$\delta_{\sigma} = \mathrm{d}\sigma\,\frac{\partial}{\partial\sigma} \qquad \nabla_{\sigma} = \nabla_{z} + \boldsymbol{S}\,\partial_{z} \qquad \boldsymbol{S} = \nabla_{\sigma}z = -z_{\sigma}\nabla_{z}\sigma \qquad J^{\sigma} = z_{\sigma}\nabla\sigma\cdot\boldsymbol{J} \qquad (17)$$

Scalar equations with vertical Lagrangian remapping

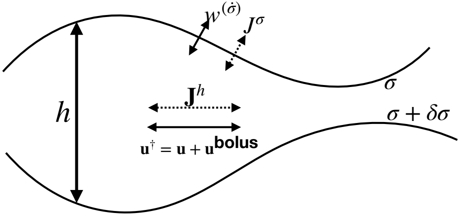

- Vertical advection from $w^{(\dot\sigma)}$ is handled during the remap step.
- Vertical parameterized advection from $w^{(*\dot\sigma)}$ is handled during the Lagrangian step via the horizontal convergence $-\nabla_\sigma \cdot [h\,\boldsymbol{u}^{\dagger}]$.
- Use of $\boldsymbol{u}^{\text{bolus}}$ ensures that horizontal advective transport retains constant layer integrated mass just as in an adiabatic isopycnal layer.

$$\frac{\partial (h\,\rho)}{\partial t} + \nabla_\sigma \cdot (h\,\rho\,\boldsymbol{u}^{\dagger}) + \delta_\sigma(\rho\,w^{(\dot\sigma)}) = 0 \tag{18}$$

$$\frac{\partial (h\,\rho\,C)}{\partial t} + \nabla_\sigma \cdot (h\,\rho\,C\,\boldsymbol{u}^{\dagger}) + \delta_\sigma(\rho\,C\,w^{(\dot\sigma)}) = -\left[\nabla_\sigma \cdot (h\,\boldsymbol{J}^h) + \delta_\sigma J^\sigma\right] \tag{19}$$

$$w^\sigma = \frac{\partial z}{\partial \sigma}\frac{\mathrm{D}\sigma}{\mathrm{D}t} \qquad \boldsymbol{u}^{\dagger} = \boldsymbol{u} + \boldsymbol{u}^{\text{bolus}} = \text{horizontal residual mean velocity.} \tag{20}$$

Outline

3. Closing comments

Choice of vertical coordinate matters for heat uptake!

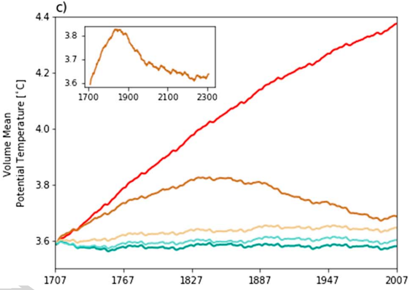

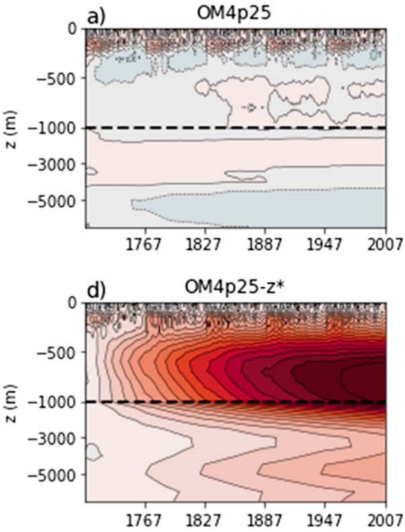

- ⋆ MOM6/SIS2 at $0.25^\circ \times 75$-layers forced by interannual CORE.
- ⋆ z^* dominated by spurious mixing relative to hybrid isopycnal-z^*.

Summary points

- ⋆ We understand a great deal about ocean mixing and how to parameterize it. However, spurious numerical diapycnal mixing remains a nontrivial problem with many simulations that can corrupt their physical fidelity.
- ⋆ There are a handfull of methods for diagnosing spurious mixing. They all point to the need for improved numerical accuracy and maintenance of modest [$\mathrm{Re}_{\mathrm{grid}} < \mathcal{O}(10)$] grid Reynolds number.
- ⋆ Vertical Lagrangian-remapping offers a framework for incorporating hybrid/generalized vertical coordinates.
- ⋆ The design of hybrid coordinates should be targeted at minimizing spurious diapycnal mixing while allowing for an accurate representation of the ocean's multiple regimes of flow.
- ⋆ More work is needed to improve the choice for vertical coordinate, with no optimal coordinate having been found that satisfies all needs (sometimes subjective needs) for climate and coastal applications.

PRINCETON UNIVERSITY

Many thanks for your time and attention

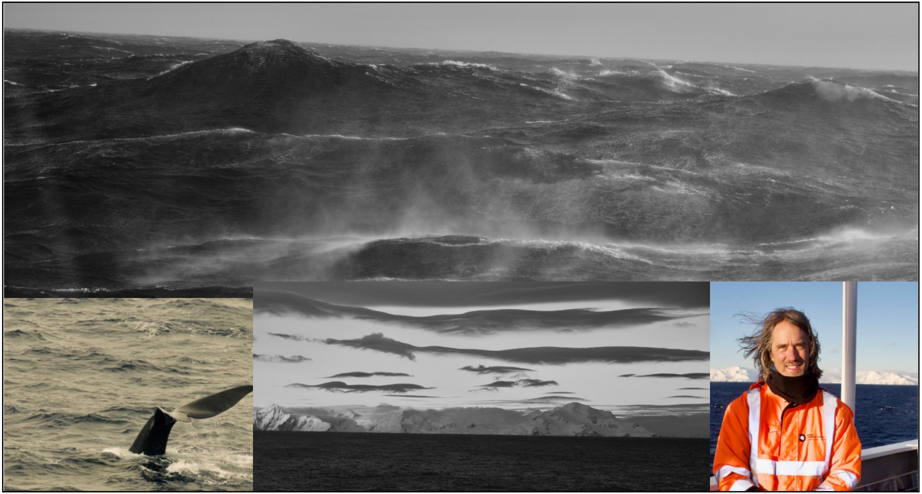

From the Weddell Sea and Scotia Sea, autumn 2017 on the RRS James Clark Ross

PRINCETON UNIVERSITY